International Journal of Pharmaceutics 471 (2014) 312–321

Contents lists available at ScienceDirect

International Journal of Pharmaceutics

journal homepage: www.elsevier.com/locate/ijpharm

Linolenic acid-modified PEG-PCL micelles for curcumin delivery

Zhimei Song [a], Wenxia Zhu [b,c], Na Liu [a], Fengying Yang [a], Runliang Feng [a,*]

[a] Department of Pharmaceutical Engineering, School of Biological Science and Technology, University of Jinan, 336 Nanxinzhuang Xilu, Jinan, Shandong Province 250022, PR China
[b] School of Medicine and Life Sciences, University of Jinan, 336 Nanxinzhuang Xilu, Jinan, Shandong Province 250022, PR China
[c] Shandong Academy of Medical Sciences, 18877 Jingshi Road, Jinan, Shandong Province 250062, PR China

ARTICLE INFO

Article history:
Received 10 January 2014
Received in revised form 1 May 2014
Accepted 29 May 2014
Available online 2 June 2014

Keywords:
Linolenic acid
Curcumin
PEG-PCL
Micelles

ABSTRACT

In this study, a novel linolenic acid-modified poly(ethylene glycol)-b-poly(ε-caprolactone) copolymer was prepared through radical addition, ring-opening polymerization, and *N*-acylation reactions. Its structure was characterized by ^{1}H NMR and GPC. Micelles were developed by thin-film hydration and used as a delivery system for curcumin with high drug loading capacity of 12.80% and entrapment efficiency of 98.53%. The water solubility of curcumin was increased to 2.05 mg/mL, which was approximately 1.87×10^5 times higher than that of free curcumin. The micelles were spherical shape with an average diameter of 20.8 ± 0.8 nm. X-ray diffraction and FT-IR studies suggested that curcumin existed in the polymeric matrices under π–π conjugation and hydrogen bond interaction with the copolymer. *In vitro* drug release studies indicated that the curcumin release from linolenic acid-modified copolymer micelles met controlled release, and its release rate was less than that from the linolenic acid-unmodified copolymer micelles. Cytotoxicities against Hela and A-549cells demonstrated that the additional π–π conjugation could affect curcumin's anticancer activity through reducing its release from micelles. Hemolysis test and intravenous irritation test results revealed that the linolenic acid-modified copolymer was safe for intravenous injection. The plasma $AUC_{0-\infty}$ and $MRT_{0-\infty}$ of curcumin-loaded linolenic acid-conjugated poly(ethylene glycol)-b-poly(ε-caprolactone) copolymer micelles were 2.75- and 3.49-fold higher than that of control solution, respectively. The CL_z was also decreased by 2.75-fold. So, this linolenic acid-modified copolymer might be a carrier candidate for curcumin delivery.

1. Introduction

Curcumin (CUR) is a low-molecular-weight, natural polyphenolic compound isolated from the rhizome of turmeric (*Curcuma longa*). It has a low intrinsic toxicity with anti-oxidative, -inflammatory, -microbial, and -tumor properties (Maheshwari et al., 2006; Ono et al., 2004). Preclinical studies of CUR have shown its ability to inhibit a variety of cancer cell lines (Aggarwal et al., 2003). The ability of CUR to induce apoptosis in cancer cells without cytotoxic effects on healthy cells makes it a potential compound against cancer (Aggarwal et al., 2003; Hatcher et al., 2008). However, its clinical potential has been greatly limited due to extremely low solubility in aqueous solution (2.99×10^{-8} M) as well as its poor bioavailability (Letchford et al., 2008).

Micelles are extensively researched as drug delivery systems, which have several advantages such as small size particles, ease of administration, drug targeting to the specific issues, solubility of hydrophobic drugs (Grottkau et al., 2013). Poly(ethylene glycol) (PEG), a hydrophilic polymer, can avoid to phagocytosis of reticulo-endothelial system (RES) and prevent hydrophobic compounds from the absorption of blood proteins to prolong their cycling time *in vivo* (Wang et al., 2011; Wei et al., 2012; Zhang et al., 2011). Hydrophobic poly(D,L-lactide) (PLA) (Tu et al., 2007), poly(ε-caprolactone) (PCL) (Jia et al., 2008), poly(δ-valerolactone) (Nair et al., 2011) (PVL), and poly(glycolide) (PGA) (Ding et al., 2012) have been coupled with PEG to form amphiphilic copolymer, respectively. These copolymers are biodegradable and biocompatible, which have distinct hydrophilic and hydrophobic segments forming an inner core and outer shell due to their large solubility difference in aqueous medium. They have been used to encapsulate lipid drugs under hydrophobic interactions to enhance drug's solubility or activity (Gao et al., 2009; Hu and Zhang, 2010), change drug's crystalline state (Shin et al., 2010; Zhang et al., 2010b), and improve controlled release property (Derakhshandeh et al., 2010; Hu and Zhang, 2010). For example, methoxy PEG-PCL diblock copolymer can successfully encapsulate CUR with a higher drug loading capacity, improving CUR's solubility,

* Corresponding author. Tel.: +86 531 89736825; fax: +86 531 89736818.
E-mail address: runliangfeng@126.com (R. Feng).

http://dx.doi.org/10.1016/j.ijpharm.2014.05.059
0378-5173/

pharmacokinetics property or anticancer activity (Chen et al., 2011; Gong et al., 2013; Kanazawa et al., 2011; MaLing et al., 2011; Shao et al., 2011; Yin et al., 2013).

It is noted that modification of PEG with long-chain fatty acid also forms a typical core-shell type structure for encapsulating clonazepam into inner core and showing controlled release (Lee et al., 2003). Furthermore, linolenic acid (LNA) has several conjugated double bonds which can interact with aromatic cycle or other conjugated bond *via* π–π orbital overlapping (Heard et al., 2005). Consequently, compared with PEG-PCL without LNA (NH_2-PEG-PCL), it is believed that LNA-modified PEG-PCL (LNA-PEG-PCL) can afford additional π–π orbital overlapping interaction with CUR, a polyphenolic compound containing a large conjugation system. This additional π–π orbital overlapping interaction should strengthen the encapsulation of CUR into the inner core in aqueous medium.

The main objective of this study is to investigate the feasibility of LNA-PEG-PCL micelles as a drug carrier for anticancer drugs. This copolymer was synthesized and characterized by ^{1}H NMR and GPC. Its biocompatibility was evaluated by use of hemolysis test. Curcumin's physical state and *in vitro* release kinetics from the LNA-PEG-PCL micelles were studied. We also performed *in vitro* cytotoxicity tests to investigate effects of LNA modification of PEG-PCL on cytotoxicity against Hela and A-549cancer cell lines.

2. Materials and methods

2.1. Materials

CUR was purchased from Fluka Chemical Company Inc. (Buchs, Switzerland). Allyloxy poly(ethylene glycol) (APEG) (Mn = 2400) was procured from Sungder Chemical (Nantong) Co., Ltd. (Nantong, Jiangsu Province, China) and dried twice by azeo-distillation of toluene. ε-Caprolactone (ε-CL) was provided by Huayuan polymer Co. Ltd. (Qingdao, Shandong Province, China). Cysteamine hydrochloride purchased from Xinhaihong Chemical Industry Co., Ltd. (Hangzhou, Zhejiang Province, China) was dried by use of silica gel in desiccators for 48 h. 2,2′-Azobisisobutyronitrile (AIBN) was bought from Damao Chemical Reagent Factory (Tianjin, China). Methylene dichloride and *N*,*N*-dimethyl formamide (DMF) were dried by 4 A molecular sieves. Ethyl linolenate was bought from Linuo Biochemistry Co., Ltd. (Anyang, Henan Province, China). All the other chemicals and solvents were of analytical grade or higher, obtained commercially.

2.2. Synthesis of H_2N-PEG

The H_2N-PEG was synthesized based on a methodology reported about H_2N-PEG-N_3 (Hiki and Kataoka, 2007). A 500 mL three-neck flask equipped with a magnetic stirring bar was charged with APEG2400 (12 g, 5 mmol), cysteamine hydrochloride (11.35 g, 100 mmol), AIBN (0.82 g, 5 mmol), and 250 mL of dried DMF. The mixture was stirred at 65–70 °C for 24 h under nitrogen flow. The solvent was removed by rotary evaporation under vacuum. The residual solid was treated with 1 mol/L potassium carbonate solution (100 mL), evaporated to dry, dissolved in methylene dichloride (150 mL), and filtered in turns. The filtrate was concentrated to 1/10 of the initial volume. After precipitated from an excess volume of diethyl ether, the H_2N-PEG polymer was obtained (10.9 g, yield 88%). ^{1}H NMR ($CDCl_3$): δ1.82–1.91(2H, m, S—CH_2**CH_2**CH_2—O), 2.64(2H, t, S—**CH_2**CH_2CH_2—O), 2.75(2H, t, NH_2CH_2**CH_2**—S-$CH_2CH_2CH_2CH_2$—O), 3.03 (2H, t, NH_2**CH_2**CH_2—S-$CH_2CH_2CH_2CH_2$—O), 3.39–3.89 (218H, m, O**CH_2-CH_2**O).

2.3. Synthesis of H_2N-PEG-PCL diblock copolymer

The H_2N-PEG-PCL diblock copolymer was synthesized through a previously published method of MPEG-PVL copolymer (Lee et al., 2005) and PCL-PPG-PCL preparation (Oh et al., 2009). To remove the last traces of water, H_2N-PEG (12.4 g, 5 mmol) was azeotroped with toluene (50 mL) at 120 °C for 4 h in a 100 mL three-neck flask. The toluene was removed by evaporation. To the residual dicloromethane (200 mL), 1 mol/L hydrochloride ethyl ether (10 mL) and different weight of ε-CL were added in turns. The reaction mixture was stirred at 25 °C for 24 h. The resultant mixture was evaporated under vacuum and precipitated in 100 mL of diethyl ether. The H_2N-PEG-PCL diblock copolymer was obtained after filtration and drying under atmosphere. ^{1}H NMR ($CDCl_3$): δ1.33–1.43(48H, m, OOC—CH_2CH_2**CH_2**CH_2CH_2O), 1.56–1.70(96H, m, OOC—CH_2**CH_2**CH_2**CH_2**CH_2O), 2.29–2.34(48H, m, OOC—**CH_2**$CH_2CH_2CH_2CH_2$O), 2.5–2.95(6H, m, NH_2**CH_2CH_2**—S-**CH_2**$CH_2CH_2CH_2$—O), 3.65(218H, m, O**CH_2CH_2**O), 4.04–4.08(48H, t, OOC—$CH_2CH_2CH_2CH_2$**CH_2**O).

2.4. Synthesis of LNA-PEG-PCL diblock copolymers

The ethyl linolenate (3.06 g, 10 mmol) dissolved in methanol (50 mL) was mixed with 5 mol/L sodium hydroxide (4 mL, 20 mmol) and stirred for 24 h at room temperature. The solvent was evaporated under vacuum. The residue was dissolved in methylene dichloride, washed with water to neutral, dried with anhydrous sodium sulfate and evaporated in vacuum to obtain LNA.

LNA (556 mg, 2 mmol) and *N*,*N*-dicyclohexyl carbamide (494 mg, 2.4 mmol) were dissolved in methylene dichloride (30 mL) and agitated for 0.5 h at room temperature. To the mixture, *N*,*N*-dimethylamine pyridine (12.2 mg, 0.1 mmol) and different molecular weight of H_2N-PEG-PCL (1.8 mmol) were added and continuously stirred for 24 h at the same temperature. The reaction mixture was filtered to remove formed precipitate, evaporated under vacuum to dry and precipitated with ethyl ether to gain LNA-PEG-PCL. ^{1}H NMR ($CDCl_3$): δ0.95–1.00(3H, t, CH_3CH_2 of LNA), 1.31–1.43(58H, m, OOC—CH_2CH_2**CH_2**CH_2CH_2O), 1.60–1.70(106H, m, OOC—CH_2**CH_2**CH_2**CH_2**CH_2O of PCL and 3-CH_2 to 7-CH_2 of LNA), 2.07(4H, t, 8-CH_2 and 17-CH_2 of LNA), 2.28–2.33 (50H, m, OOC—**CH_2**$CH_2CH_2CH_2CH_2$O of PCL and 2-CH_2 of LNA), 2.82(4H, m, 11-CH_2 of LNA and $NHCH_2$**CH_2**-SCH_2), 3.64(218H, m, O**CH_2CH_2**O of PEG), 4.04–4.08(48H, t, OOC—$CH_2CH_2CH_2CH_2$**CH_2**O), 4.22(2H, t, terminal CH_2 of PEG).

2.5. Preparation of micelles

Micelles were prepared by thin-film hydration (Wang et al., 2012). CUR and copolymer (1:7 (w/w)) were co-dissolved in acetone in a round-bottomed flask to form a clear solution. A yellowish thin layer of uniform film on the wall of flask formed under vacuum rotary evaporation. The resulting thin film was hydrated in 5 mL water with moderate rotating at 65 °C, filtered through a 0.22 μm filter membrane to remove non-incorporated drugs and copolymer aggregates and used for further analysis or lyophilization. Bank micelles were prepared in a similar approach.

The accurate volume of drug-loaded micelles solution was added into ethanol in a 10 mL of volumetric flask to disrupt the micelles' core-shell structure and dissolve CUR releasing from the micelles. Through stepwise dilution, a solution of CUR with UV absorbance at a range of 0.2–0.8 was provided. The CUR content in the drug-loaded micelles was determined using the UV–vis spectrophotometer at 425 nm. The drug loading content (DL) and drug encapsulation efficiency (EE) were calculated based on the following formula (Song et al., 2011):

$$EE = \frac{\text{Weight of drug in nanoparticles}}{\text{Weight of the initial drug}} \times 100\%$$

$$DL = \frac{\text{Weight of drug in nanoparticles}}{\text{Weight of nanoparticles containing drug}} \times 100\%$$

2.6. Charaterization of micelles' physico-chemical properties

2.6.1. Morphology of CUR-loaded LNA-PEG-PCL (CUR-LNA) micelles

Transmission electron microscope (TEM, JEM-1200EX, JEOL, Tokyo, Japan) was used for morphological observation. One drop of micelles solution was placed on a carbon film-coated copper grid of 400 meshes. After negative staining with 2% phosphotungstic acid for 20 s, the excess solution was absorbed by filter paper and dried in air before analysis.

2.6.2. Particle size and zeta potential of blank LNA-PEG-PCL (blank LNA) and CUR-LNA micelles

Particle size and its distribution (expressed as polydispersity index, PDI) of blank LNA and CUR-LNA micelles were determined by dynamic light scattering (DLS, Zetasizer 3000HS, Malvern Instruments Ltd., UK). The micelles were suspended in deionized water before measurement under a fixed scattering angle of 90° at 25 °C in the condition of He–Ne laser (633 nm). The surface charge of the drug-free and -loaded micelles suspension in deionized water was estimated by Laser Doppler Anemometry (Zetasizer 3000HS, Malvern Instruments Ltd., UK). Results were expressed as mean ± standard deviation (SD). All the measurements were analyzed in triplicates.

2.6.3. X-ray diffraction (XRD) and FT-IR studies of CUR, blank LNA and CUR-LNA micelles

XRD analysis was used to confirm if CUR exists in the crystallographic form in the nanoparticulate CUR formulation or not. The XRD patterns of CUR, blank LNA and CUR-LNA micelles were obtained from X-ray diffractometer measurements (Bruker D8 Focus, Bruker, Germany). The measurements were performed at a voltage of 40 kV and 25 mA using Cu Kα radiation. The scanned angle was set from 1.7° to 40°, and the scan rate was 2°/min.

FT-IR spectra were also done to research the possible physical and chemical interactions between the CUR and the polymer matrix. FT-IR spectrum of the CUR, lyophilized blank LNA, and CUR-LNA micelles was obtained by KBr pellets method on a FT-IR spectrometer (Spectrum One, PerkinElmer, USA), respectively. The wavenumber range was set from 4000 to 400 cm^{-1}.

2.6.4. Hemolysis test of copolymers

Hemolysis assay was performed using a method formerly elaborated to evaluate the copolymer's biocompatibility (Meng et al., 2011). Briefly, heparinized rat erythrocytes were separated from 5 mL of rat blood by centrifugation at 3000 rpm for 30 min in a centrifuge (TG16-WS, Xiangyi instrument Co. Ltd., Xiangtan, Hunan Province, China) and washed with physiological saline to achromatic color for supernatant solution. 1 mL of the purified erythrocytes was mixed with 39 mL of normal saline to form a 2.5% erythrocytes suspension (v/v). 1.6 mL of the resulting suspension was mixed with 4 mL of copolymers' solution in normal saline prior to shaking incubation for 30 min at 37 °C in an oscillator (SHZ-88, Jintan Medical Instrument Factory, Jintan, Jiangsu Province, China). The copolymer concentration range was set from 156 to 2500 μg/mL. Physiological saline and distilled water were used as negative and positive control, respectively. After incubation, the samples were centrifuged for 20 min at 8000 rpm/min for the purpose of isolating unbroken erythrocytes and disrupted membranes from the solution. The supernatant, containing the released hemoglobin (Hb), was collected. The absorbance of Hb in the supernatant at 500–650 nm was measured by UV–vis spectrophotometer (T6 New Century, Purkinje General, Peking, China).

The degree of hemolysis was determined on the basis of absorbance at 576 nm and calculated from the following formulation (Dutta and Dey, 2011):

$$\text{Hemolysis}(\%) = \frac{\text{Abs}_{\text{sample}} - \text{Abs}_{\text{negative control}}}{\text{Abs}_{\text{positive control}} - \text{Abs}_{\text{negative control}}} \times 100\%$$

where $\text{Abs}_{\text{sample}}$, $\text{Abs}_{\text{negative}}$, and $\text{Abs}_{\text{positive}}$ were absorbance of copolymer sample, physiological saline (0% hemolysis) and distilled water (100% hemolysis). All assays were performed in triplicate.

2.6.5. Intravenous irritation test

One New Zealand rabbit with weight of 2.0–2.5 kg was injected with a daily dose of 15 mg/kg of CUR-LNA micelles solution and equivalent volume of physiological saline into the right and left ear-border vein at an injection rate of 1 mL/min for 3 days, respectively (Jing et al., 2014). After injection, pathological reaction at the injection site was recorded. The rabbits were sacrificed by bleeding 24 h after the last administration. At the localizations of 1.3 cm from the injection site to proximal part, the ears were cut and fixed in 10% formalin for histological observation.

2.7. In vitro *release of CUR-LNA micelles*

In vitro drug release profile of CUR from CUR-LNA micelles was done by dynamic dialysis method previously reported with a solution of ethanol-normal saline (40:60) as release medium(Sun et al., 2012). CUR-LNA micelles and CUR-loaded NH_2-PEG-PCL micelles (CUR micelles) control solution containing 1 mg of CUR were put into dialysis bags (Viskas MD25-3.5, Union Carbide Corporation, Bound Brook, NJ, USA) with a 3500 Da molecular cut-off, respectively. The bags were placed into 100 mL release mediums in a beaker and vibrated with 100 rpm/min of oscillation at 37 °C. At definite time intervals, 5 mL of the release mediums was withdrawn. The same volume of fresh release mediums was supplemented to maintain a constant volume. The release amount of drug was quantified spectrophotometerically at a wavelength of 425 nm. All experiments were performed in triplicates. The release rate was calculated from the following equation, and the results were expressed as mean ± SD:

$$Q_n = C_n V_0 + \sum_{i=0}^{n-1} C_i V_i$$

$$R(\%) = \frac{Q_n}{W} \times 100\%$$

where Q_n is the accumulative released amount of drug, C_n is the drug concentration in the release medium of each time interval, V_0 is the total volume of the release medium, V_i is the volume of the withdrawn medium, C_i is the drug concentration in the release medium at time i, R is the abbreviation of accumulative release percentage, and W is the total drug weight in each dialysis bags.

2.8. In vitro *cytotoxicity of micelles*

The HeLa and A-549cells were cultured in Dulbecco's modified Eagle's medium supplemented with 10% fetal bovine serum (FBS) in 24-well plate. Then, all cells were incubated for 24 h in incubator (37 °C, 5% CO_2). The culture medium was removed, and fresh couture medium containing different dosages of CUR, blank micelles, CUR micelles, blank LNA micelles, or CUR-LNA micelles

was added each well, respectively. Cells were co-incubated at 37 °C for 48 h. The drug dosages were set as 0, 5, 10, 20 and 40 μmol/L, respectively. The blank copolymer concentration was the same as the corresponding curcumin-loaded micelles. The culture medium without treatment was used as control group. For cytotoxicity assay after incubation for 48 h, the culture medium containing micelles was displaced by 90 μL of fresh culture medium, and 10 μL of MTT solution (5 mg/mL) was added to each well, and the plates were incubated for 4 h. The medium was removed, and the MTT formazan crystals were then dissolved with 1 mL of DMSO at ambient temperature. The optical density was measured at 490 nm with a spectrophotometer (Multiskan GO 1.00.40, Thermo Scientific). The viable rate was determined by comparing the absorption at 490 nm with control wells containing only cell culture medium (Rezaei et al., 2012). The experiments were performed in triplicates.

2.9. Pharmacokinetics of CUR-LNA micelles

Animal experiments were conducted in full compliance with national regulatory principles. Male Sprague–Dawley rats (250 ± 20 g) were supplied by the center for new drug evaluation Shandong University (Shandong, China). The rats were housed under standard conditions of temperature, humidity and light, and took standard rodent diet and water freely ahead of each experiment. The rats fasted overnight prior to drug dosing.

Free CUR was completely dissolved in a solution being made up of *N*,*N*-dimethyl acetamide (15%, v/v), PEG-400 (45%, v/v) and 5% glucose solution (40%, v/v) to afford CUR control (Song et al., 2011).

Two groups of rats (six/group) were given CUR control or CUR-LNA micelles at 15 mg/kg *via* the tail veins injection, respectively. After drug administration, blood samples were withdrawn into heparinised centrifugal tubes and centrifuged at 3000 rpm/min for 10 min for plasma separation at the definite time. The gathered plasma was stored at −20 °C prior to analysis. The treatment of plasma samples was performed according to a method described previously (Song et al., 2011). A Shimadzu LC-10A HPLC system equipped with a UV detector was used to determine quantitatively the concentration of CUR in plasma samples at 425 nm. The mobile phase contained a 52% acetonitrile and 48% citric acid buffered solution (pH 3.0, v/v). The flow rate was set at 1 mL/min. The injection volume for all samples was 5 μL.

The plasma concentration *vs.* time profile for each rat was analysed using DAS 2.0 software to evaluate the pharmacokinetic parameters *via* non-compartmental model analysis.

3. Result and discussion

3.1. Synthesis and characterization of LNA-PEG-PCL

In a former article, the H_2N-PEG-PCL diblock copolymer is synthesized by radical addition reaction of cysteamine hydrochloride and allyl-PEG-PCL under AIBN as catalyst (Feng et al., 2013). However, there may be ammonolysis side-reaction of PCL chain in this reaction. In this article, H_2N-PEG was firstly prepared from radical addition reaction of APEG with cysteamine hydrochloride, then the pure H_2N-PEG-PCL diblock copolymer was synthesized through ring-opening copolymerization reaction of ε-CL with H_2N-PEG because amino group showed different reaction activity from hydroxyl group in H_2N-PEG under hydrochloride diethyl ether as catalyst (Fig. 1). The LNA-PEG-PCL was prepared from *N*-acylation reaction of H_2N-PEG-PCL diblock copolymer with LNA in condition of DCC as condensation reagent and DMAP as catalyst (Fig. 1).

The ^{1}H HMR spectrum of H_2N-PEG was listed in Fig. 2A; the signals were clearly observed at 1.82–1.91 (d, $OCH_2CH_2CH_2S$), 2.62 (c, $OCH_2CH_2CH_2S$), 2.75 (b, $SCH_2CH_2NH_2$), and 3.03 ppm (a, $CH_2SCH_2CH_2NH_2$) corresponding to the resulting structure *via* the radical addition of 2-aminoethanethiol to allyl group of APEG shown as Fig. 1. The corresponding signals were similar to that of H_2N-PEG-N_3 reported by Hiki (Hiki and Kataoka, 2007).

The LNA-PEG-PCL was analyzed by ^{1}H HMR (Fig. 2C). The peak at 0.95–1.00 (j) originated from methyl group of linolenyl, and the peaks at 1.60–1.70 (o–s), 2.07 (k + n), 2.28–2.33 (t) and 2.82 (m) were assigned to methylene groups of linolenyl at 3- to 7-, 8-, 17-, 2- and 11-positions, respectively (Fig. 2C), which were simliar to that of LNA reported early (Crombie and Morgan, 1991). The characteristic GPC curve of LNA-PEG_{2400}-PCL_{2400} is shown as Fig. 3. The monopeak indicated that the LNA-PEG-PCL copolymeer was prepared without any other side reactions.

3.2. Characterization of micelles

The LNA-PEG-PCL copolymer contained hydrophilic PEG and hydrophobic PCL or LNA. It is thought that the copolymer can also self-assembly form a core-shell structure in aqueous medium. The hydrophilic core's interaction with hydrophilic drug results in increasing drug's water-solubility, but its percentages in the copolymer have important effect on improving drug's water solubility when the molecular weight of PEG is constant (Lee et al., 2005; Sun et al., 2013). So, in order to gain an ideal drug formulation, we researched the effect of PCL chain length on curcumin's encapsulation efficiency (EE) when molecular weight

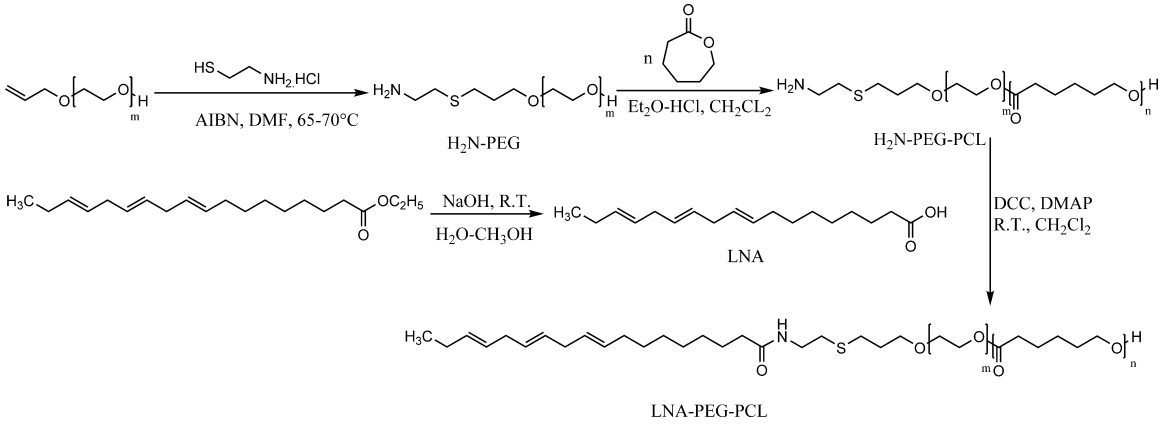

Fig. 1. Synthesis scheme of LNA-PEG-PCL.

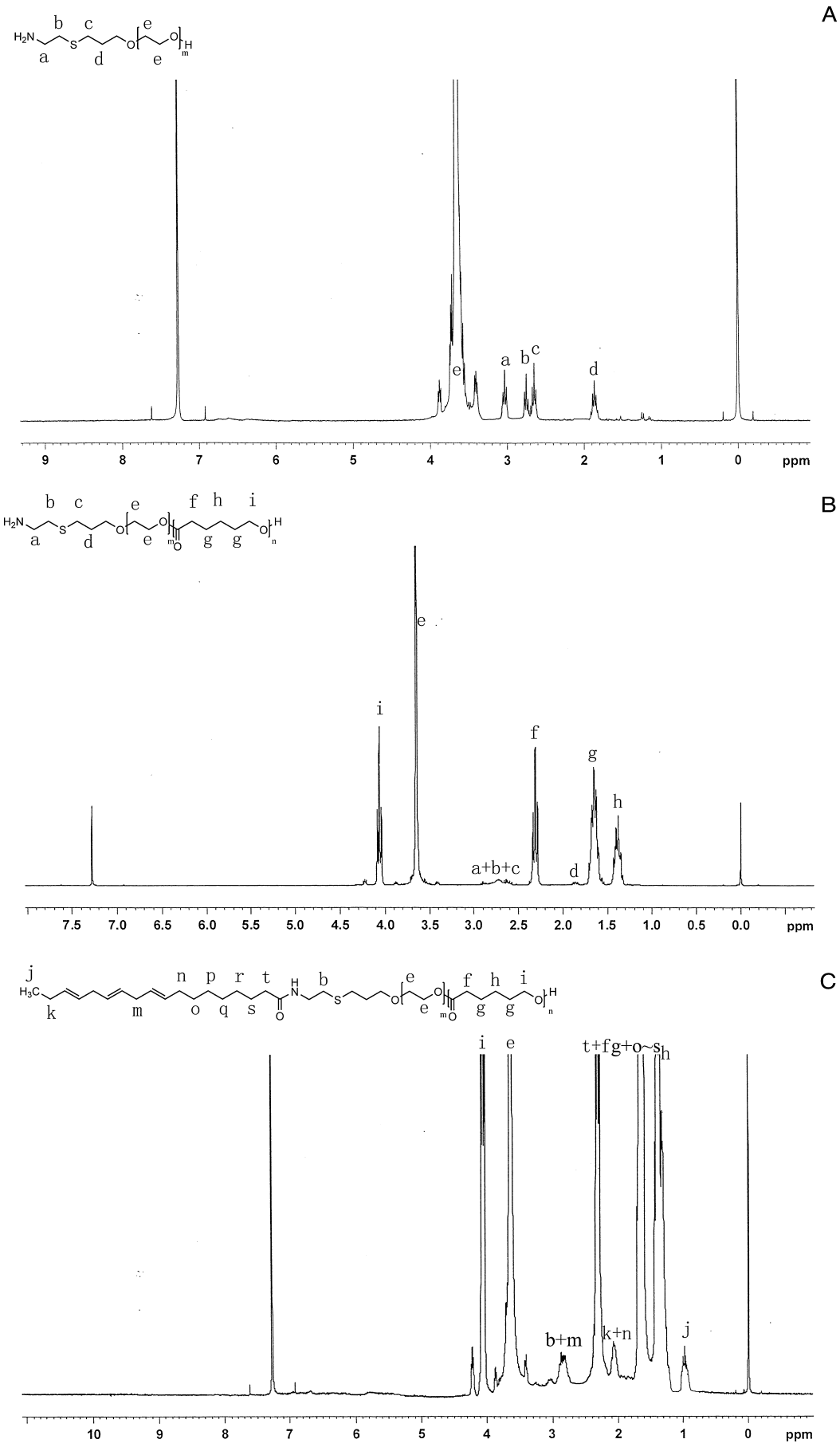

Fig. 2. ^{1}H HMR spectrum of H_2N-PEG (A), H_2N-PEG-PCL (B) and LNA-PEG-PCL (C).

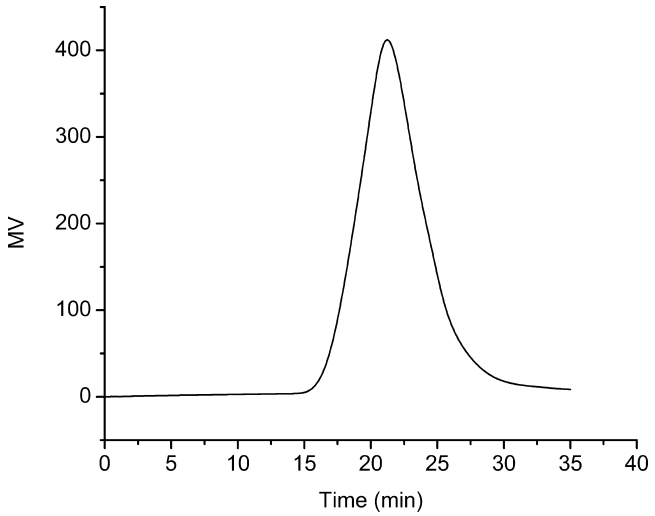

Fig. 3. GPC of LNA-PEG_{2400}-PCL_{2400}.

of PEG was constant. As shown in Table 1, the EE was 96.60 ± 2.16% for LNA-PEG_{2400}-PCL_{1200}, which was similar to LNA-PEG_{2400}-PCL_{2400}, but the former copolymer was unstable and precipitated when stored in 4 °C refrigerator. By contrast, the EE obviously decreased for LNA-PEG_{2400}-PCL_{4800}. This might be relative to the copolymer's hydrophobic properties and interaction with drug. The hydrophobic interaction would be in favor of increasing CUR's solubility in water, but the length of hydrophobic PCL must be suitable. The CUR's solubility in water would be decreased when the length of PCL exceed a limitation. The LNA-PEG_{2400}-PCL_{2400} was selected to be studied in depth on the basis of higher EE.

In this study, UV–vis spectrophotometer was selected for quantitative analysis of CUR (without results shown). The total volume of CUR-NP solution was 4.8 mL. The DL and EE of CUR-LNA micelles prepared from LNA-PEG-PCL were 12.80% and 98.53%, respectively. So the water solubility of CUR was increased to 2.05 mg/mL, which was 1.87×10^5 times higher than that of CUR in water (Letchford et al., 2008).

The mean particle diameters of blank and CUR-loaded LNA-PEG_{2400}-PCL_{2400} micelles measured from the dynamic light scattering were 19.5 ± 2.1 nm and 20.8 ± 0.8 nm, respectively. The drug was loaded into micelles, resulting in an increase on the mean particle diameter. Zeta potentials of blank and CUR-loaded LNA-PEG_{2400}-PCL_{2400} micelles were −2.63 ± 0.17 mV and −2.12 ± 0.09 mV, respectively. This result indicated that the micelles were nearly neutral. Surface morphology of the CUR-loaded LNA-PEG_{2400}-PCL_{2400} micelles was examined by TEM. Fig. 4 shows the TEM image of the CUR-LNA micelles. The particles seemed to have a spherical shape and a smooth surface. The TEM image further confirmed the particle size detected from the dynamic light scattering.

FT-IR spectroscopy was performed to ascertain the formation of CUR-LNA micelles. Fig. 5 shows the FT-IR spectrum of CUR, blank LNA and CUR-LNA micelles. The FT-IR spectrum of blank LNA

Table 1
Characterization of CUR-LNA micelles.

Copolymer	Molecular weight from GPC	EE (%)	DL (%)
LNA-PEG_{2400}-PCL_{1200}	10,649	96.60 ± 2.16	11.96 ± 0.39
LNA-PEG_{2400}-PCL_{2400}	19,823	98.53 ± 1.73	12.80 ± 0.16
LNA-PEG_{2400}-PCL_{4800}	24,926	53.04 ± 0.19	6.63 ± 0.24

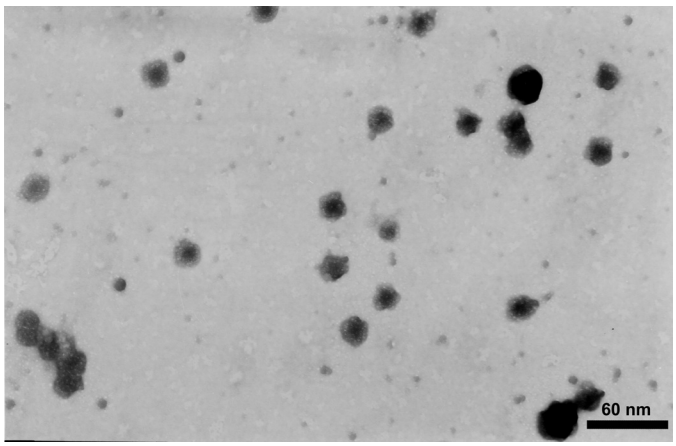

Fig. 4. TEM of CUR-LNA micelles (19000×, the scale bar is 60 nm).

micelles showed strong peaks at 2931 and 2864 cm^{-1} attributing to the stretching vibrations of *trans*-alkene C—H bonds LNA chain. Peaks at 1735 and 1702 cm^{-1} corresponded to the stretching vibrations of ester carbonyl and amide carbonyl groups, and a peak at 1657 cm^{-1} was due to C=C stretching of LNA chain. The CH_2—O—CH_2 stretching vibration and LNA's *trans*-alkene C—H deformation were found at 1108 and 1298 cm^{-1}, respectively. In micellar formulation, the wave numbers corresponding to the characteristic peaks of LNA-PEG-PCL were shifted due to the complexation of CUR with the LNA-PEG-PCL NPs. Comparing LNA-PEG-PCL with drug loaded LNA-PEG-PCL micelles, peak shifts were observed from 3448 to 3414 cm^{-1}, 1735 to 1734 cm^{-1}, 1657 to 1628 cm^{-1}, and 1298 to 1284 cm^{-1}. The blue shift of 1735–1734 cm^{-1} should be attributed to hydrogen bond between CUR and LNA-PEG-PCL copolymer (Xie et al., 2011; Yen et al., 2010).

The FT-IR spectrum of CUR exhibited an absorption band at 3509 cm^{-1} attributed to the phenolic O—H stretching vibration (Yallapu et al., 2010). Additionally, sharp absorption bands at 1627 cm^{-1} (stretching vibration of C=C bond), 1602 cm^{-1} (stretching vibrations of benzene ring), 1509 cm^{-1} (C=O and C—C vibrations), 1429 cm^{-1} (olefinic C—H bending vibration), and 1280 cm^{-1} (aromatic C—O stretching vibration) were similar to characteristic peaks of curcumin reported previously (Yallapu et al., 2010). These sharp absorption bands were also shifted to 1628, 1589, 1515, 1454, and 1284 cm^{-1} when CUR was loaded into the LNA-PEG-PCL micelles, respectively. The blue shift of stretching

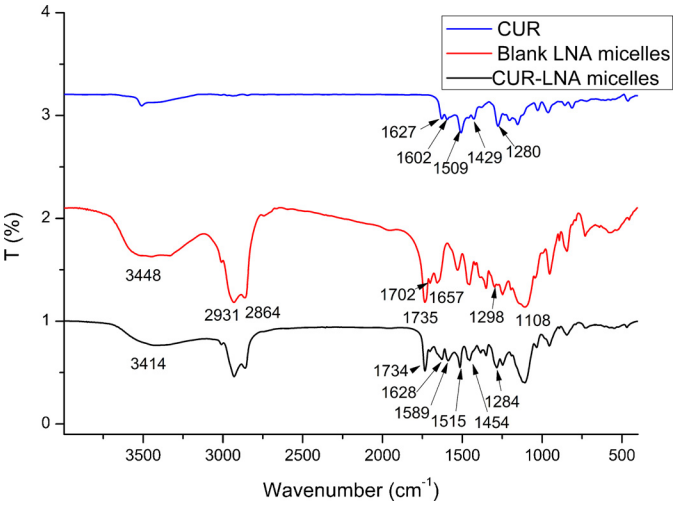

Fig. 5. FT-IR spectrum of CUR, blank LNA micelles and CUR-LNA micelles.

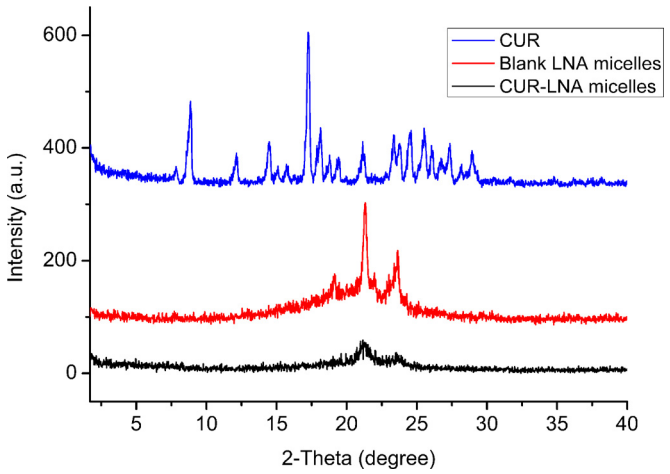

Fig. 6. XRD of CUR, blank LNA micelles and CUR-LNA micelles.

vibration of CUR's benzene ring (1602–1589 cm^{-1}) and LNA's C═C (1657–1628 cm^{-1}) was due to extension of conjugated bond caused by their π–π orbital overlapping interaction. These interactions may have effects on the *in vitro* or *in vivo* release and uptake of drug (Heard et al., 2005), and then on its activities.

XRD studies were performed to investigate the physical state of CUR in the micellar particles, because this would impact the *in vitro* and *in vivo* drug release from the micellar formulations. Fig. 6 shows the XRD diagrams of pure CUR, CUR-LNA micelles and blank LNA micelles. The pure CUR peaks at angles 2θ appeared at a series of diffraction at 8.84°, 12.14°, 14.46°, 17.26°, 18.12°, 21.14°, 23.36°, 24.50°, 25.54°, 27.34°, 28.14°, and 28.96°, which indicated that pure CUR was in a highly crystalline form (Donsi et al., 2010; Yen et al., 2010). However, these characteristic peaks did not exist in CUR-LNA micelles, showing that the state of CUR was amorphous, disordered crystalline phase or in solid solution (Anitha et al., 2011a,b,b; Zhang et al., 2010b). It is beneficial to excellent diffusion of drug molecules through the polymeric matrix, leading to a sustained release of the encapsulated drug.

Hemolysis assay will give additional information about this copolymer's biocompatibility in the case of *in vivo* application (Zobel et al., 1999). The profiles of hemolysis assay of LNA-PEG_{2400}-PCL_{2400} copolymer were shown in Fig. 7. The LNA-PEG_{2400}-PCL_{2400} exhibited hemolytic activity from 1.10% to 5.81% at the copolymer concentrations from 156 to 2500 μg/mL. The hemolytic assay indicated that LNA-PEG_{2400}-PCL_{2400} showed no obvious hemolytic activity (hemolysis percentage <5%) (Cerda-Cristerna et al., 2011).

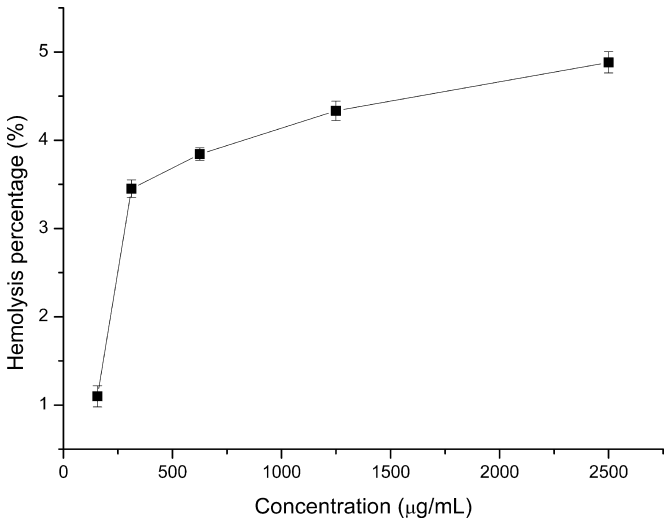

Fig. 7. Hemolysis percentage of LNA-PEG_{2400}-PCL_{2400} at different concentrations.

After the 3-day injection treatment of CUR-LNA micelles solution or physiological saline, no erythema and congestion of blood vessel were found in CUR-LNA micelles under the observation by naked eye. The microscopical observation demonstrated that vascular line and endotheliocyte structures were clear and intact, and no tissue edema and thrombus were found (Fig. 8). Furthermore, inflammatory cell infiltrate was not observed in the vessel wall and surrounding tissues. For physiological saline control, there were also no histophatological changes (Fig. 8). All the results demonstrated that CUR-LNA micelles solution at a dose of 15 mg/kg show no stimulus response in the ear vein of rabbit.

3.3. In vitro *release of CUR-LNA micelles*

The *in vitro* drug release curves of the CUR-LNA and CUR-loaded NH_2-PEG_{2400}-PCL_{2400} micelles (CUR micelles) are shown in Fig. 9. Due to the low solubility of CUR in water (Letchford et al., 2008), 40% (v/v) of ethanol saline solution was used as the dialysis medium to provide a sink condition. The drug release percentage

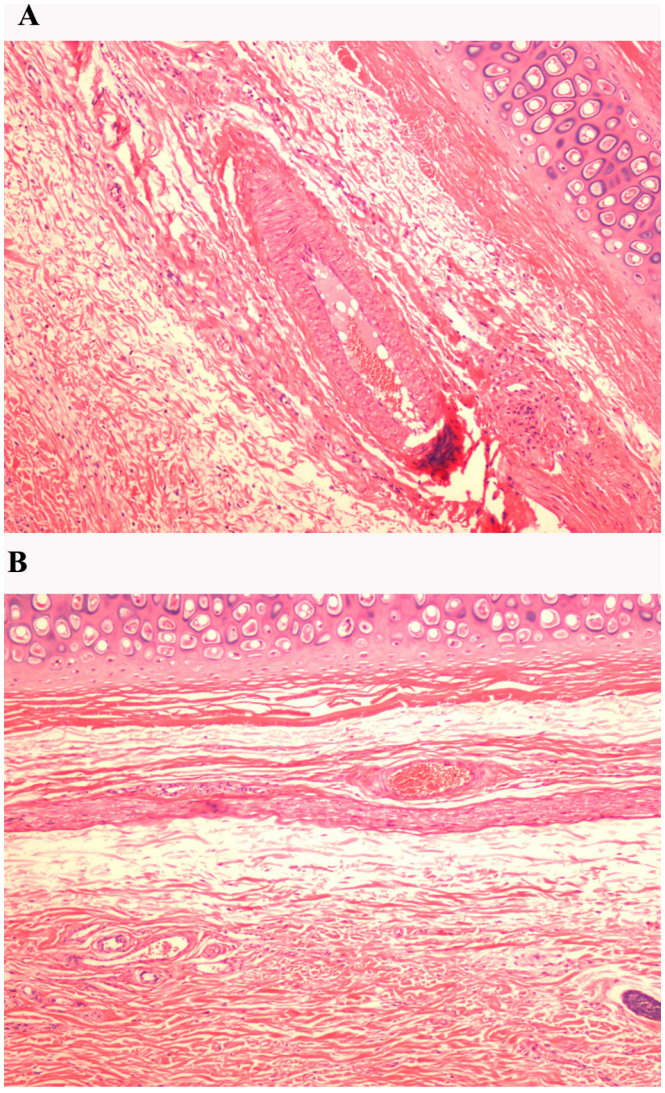

Fig. 8. Microscopical observation of vascular irritability study with different formulations of CUR-LNA micelles (A) and physiological saline (B) after administration in rabbits.

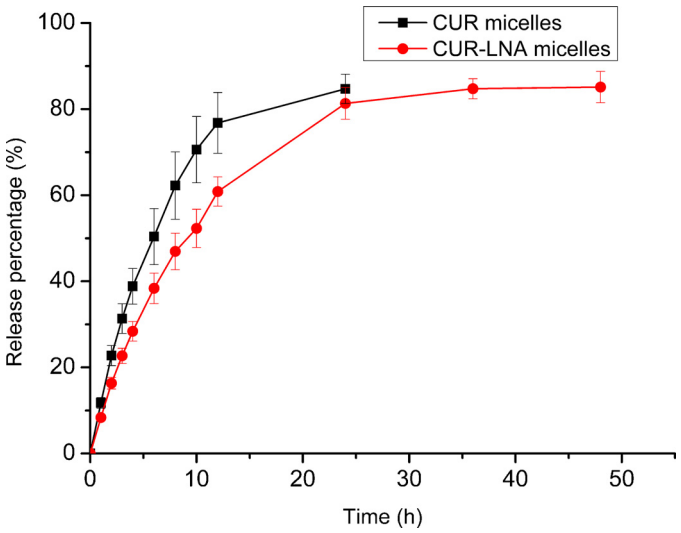

Fig. 9. *In vitro* CUR-release profile from CUR and CUR-LNA micelles in a solution of ethanol-normal saline (40:60) as release medium at 37 °C (data are presented as mean ± SD (n = 3)).

from the CUR and CUR LNA micelles was found to be 78.78% and 60.84% of the encapsulated drug during the first 12 h, respectively, while the release percentage of CUR reached 84.69% and 81.3% within following 12 h, respectively. The different release rates indicated that linolenic acid chain might interact with CUR, slowing CUR's release from CUR-LNA micelles. The initial faster drug release of micelles should be attributed to fraction of CUR loacated (or closed to) on the surface of micelles (Zhang et al., 2010a). It made CUR release faster from the LNA micelles.

3.4. In vitro *cytotoxicity of micelles*

The *in vitro* cytotoxic activity of micelles against Hela and A-549 was investigated by MTT method. After treated with blank micelles for 48 h, the two cells' viability was above 90% throughout the whole range of concentrations examined during the treatment (Fig. 10). These results showed that the CUR-free micelles did not have any obvious effect on proliferation of Hela and A-549. In other words, polymer materials had no any activities and effect on the cytotoxicity determination of CUR loaded in micelles. In the MTT experiment, CUR-LNA micelles were compared with CUR micelles to determine if LNA affected CUR's anticancer activity or not. Two kinds of CUR-loaded micelles obviously decreased the viability of Hela cells (below 48%) when the concentrations of CUR in NP were 20 μmol/L or above (Fig. 10), while they showed obvious killing function against A-549 only when CUR's concentration reached to 40 μmol/L (Fig. 10) at which the viability rate was below 48%. Certainly, CUR control showed higher activity than both of the CUR-loaded micelles in all dosages. This should be related to slower sustained release of CUR from micelles (Tao et al., 2013; Wang et al., 2012). The slower release resulted in lower concentration in cells, which showed inferior activities in comparison with CUR control. It was interesting that CUR micelles had higher activities against cancer cells than that of CUR-LNA micelles. This phenomenon should also be caused by more slower release of CUR from CUR-LNA micelles in which there were two stronger hydrogen bond (Xie et al., 2011; Yen et al., 2010) and π–π orbital overlapping (Heard et al., 2005) afforded by PEG-PCL and LNA, respectively. These interactions were confirmed by FT-IR spectrum shown in Fig. 5, and *in vitro* release results also supported that there was a causal relationship between release and anticancer activity.

3.5. Pharmacokinetics of CUR-LNA micelles

Sprague–Dawley rats were used to study pharmacokinetics of CUR-LNA micelles by intravenous route, which was also compared with CUR control solution. Fig. 11 shows the blood concentration–time curves, and Table 2 lists typical pharmacokinetic parameters of the two preparations. As shown in Fig. 11, CUR could not be detected after 1.5 h for CUR control while it could continue to exist during 6 h for CUR-LNA micelles.

The plasma concentration – time curves for CUR control and – loaded LNA micelles were all fitted to the non-compartment model. CUR-LNA micelles could distinctly chang pharmacokinetic property of CUR (Table 2). LNA micelles prolonged CUR retention in blood circulation in comparison to CUR control solution (mean retention time, $MRT_{0-\infty}$, 0.695 *vs.* 0.199 h). The half-life ($t_{1/2z}$), and

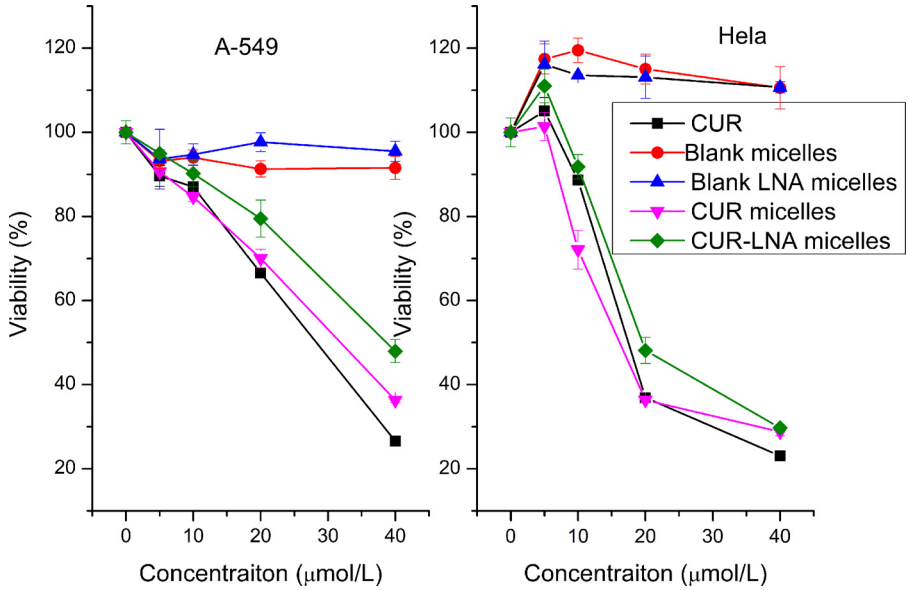

Fig. 10. *In vitro* cell cytotoxicities of CUR, blank micelles, CUR micelles, blank LNA micelles and CUR-LNA micelles against Hela and A-549cell lines (data are presented as mean ± SD (n = 3).

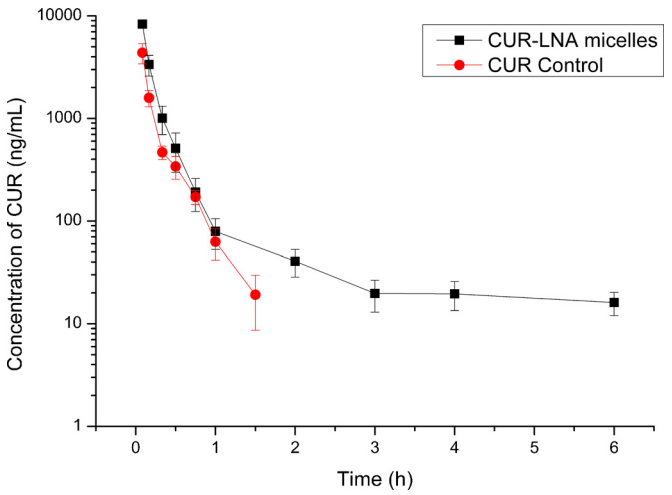

Fig. 11. The profile of concentration of CUR in plasma *vs.* time after i.v. injection of CUR control solution and CUR-LNA micelles (data are presented as mean ± SD ($n = 6$)).

Table 2
Pharmacokinetic parameters.

Parameter	CUR control	CUR-LNA-NP
$AUC_{(0-\infty)}$ (μg/L h)	967.221	2661.852
$MRT_{(0-\infty)}$ (h)	0.199	0.695
$t_{1/2z}$ (h)	0.198	3.153
CL_z (L/(h kg))	15.508	5.635
V_z (L/kg)	4.432	25.641

the area under the plasma concentration–time curve ($AUC_{0-\infty}$) of CUR in CUR-LNA micelles were 15.92- and 2.75-fold higher than those of CUR control, respectively. It was confirmed that CUR control exhibited quick metabolism and elimination in rats. In contrast, CUR-LNA micelles showed a much longer retention time in the blood circulation than CUR control. The clearance (CL_z) of CUR in CUR-LNA micelles decreased to 5.635 L/h/kg, being 2.75-fold lower than that of CUR control.

The longer $MRT_{0-\infty}$ or $t_{1/2z}$ and lower clearance manifested that the micelles could make curcumin remain in body for a longer period, which was in favor of improving CUR's distribution and therapeutic effect (Shin et al., 2010). Such long circulation time might be attributed to CUR molecules being stabilized within the micelles, preventing them from leaching and being metabolized. Such "stealth" behavior of micelles induced by their nanoscopic dimensions and the hydrophilic shell of PEG should decrease the rate of mononuclear phagocyte uptake and reduce plasma proteins absorption (Bommana et al., 2012; Shukla et al., 2012). Therefore, our data illustrated the potential utility of LNA-PEG-PCL as a drug nanocarrier with lasting circulation.

4. Conclusion

In this study, LNA-PEG-PCL was synthesized through radical addition, ring-opening polymerization and *N*-acylation with APEG as raw materials. This copolymer showed no hemolytic effect. The CUR-loaded micelles prepared by thin-film hydration with higher EE showed sustained release property *in vitro* and obviously improve CUR's solubility as well as pharmacokinetic parameters. It was worth mentioning that there was additional π–π conjugation in CUR-loaded LNA-PEG-PCL micelles in comparison with CUR-loaded H_2N-PEG-PCL micelles. This conjugation can strengthen the interaction between drug and copolymer, resulting in slower release and lower cytotoxicity of CUR. The particular structure of LNA-PEG-PCL would help to efficiently encapsulate hydrophobic drug and then change its properties *in vitro* or *in vivo*. Therefore, CUR-LNA micelles are used as an intravenously injectable aqueous formulation of CUR for anticancer application.

Conflict of interest

The authors report no conflicts of interest in this work.

Acknowledgments

This work is supported by the Excellent Young and Middle-aged Scientist Award Fund of Shandong Province, China (BS2011CL006) and Scientific Research Fund of University of Jinan (XKY1208).

Reference

Aggarwal, B.B., Kumar, A., Bharti, A.C., 2003. Anticancer potential of curcumin: preclinical and clinical studies. Anticancer Res. 23, 363–398.
Anitha, A., Deepagan, V.G., Rani, V.V.D., Menon, D., Nair, S.V., Jayakumar, R., 2011a. Preparation, characterization, in vitro drug release and biological studies of curcumin loaded dextran sulphate-chitosan nanoparticles. Carbohydr. Polym. 84, 1158–1164.
Anitha, A., Maya, S., Deepa, N., Chennazhi, K.P., Nair, S.V., Tamura, H., Jayakumar, R., 2011b. Efficient water soluble *O*-carboxymethyl chitosan nanocarrier for the delivery of curcumin to cancer cells. Carbohydr. Polym. 83, 452–461.
Bommana, M.M., Kirthivasan, B., Squillante, E., 2012. In vivo brain microdialysis to evaluate FITC-dextran encapsulated immunopegylated nanoparticles. Drug Deliv. 19, 298–306.
Cerda-Cristerna, B.I., Flores, H., Pozos-Guillén, A., Pérez, E., Sevrin, C., Grandfils, C., 2011. Hemocompatibility assessment of poly(2-dimethylamino ethylmethacrylate) (PDMAEMA)-based polymers. J. Controlled Release 153, 269–277.
Chen, C.H., Cuong, N.V., Chen, Y.T., So, R.C., Liau, I., Hsieh, M.F., 2011. Overcoming multidrug resistance of breast cancer cells by the micellar doxorubicin nanoparticles of mPEG-PCL-graft-cellulose. J. Nanosci. Nanotechnol. 11, 53–60.
Crombie, L., Morgan, D.O., 1991. Synthesis of [14,14-2H2]-linolenic acid and its use to confirm the pathway to 12-oxophytodienoic acid (12-oxoPDA) in plants: a conspectus of the epoxycarbonium ion derived family of metabolites from linoleic and linolenic acid hydroperoxides. J. Chem. Soc., Perkin Trans. 1, 581–587.
Derakhshandeh, K., Soheili, M., Dadashzadeh, S., Saghiri, R., 2010. Preparation and in vitro characterization of 9-nitrocamptothecin-loaded long circulating nanoparticles for delivery in cancer patients. Int. J. Nanomed. 5, 463–471.
Ding, G.B., Liu, H.Y., Lv, Y.Y., Liu, X.F., Guo, Y., Sun, C.K., Xu, L., 2012. Enhanced in vitro antitumor efficacy and strong anti-cell-migration activity of a hydroxycamptothecin-encapsulated magnetic nanovehicle. Chemistry 18, 14037–14046.
Donsi, F., Wang, Y., Li, J., Huang, Q., 2010. Preparation of curcumin sub-micrometer dispersions by high-pressure homogenization. J. Agric. Food Chem. 58, 2848–2853.
Dutta, P., Dey, J., 2011. Drug solubilization by amino acid based polymeric nanoparticles: characterization and biocompatibility studies. Int. J. Pharm. 421, 353–363.
Feng, K., Wang, S., Ma, H., Chen, Y., 2013. Chirality plays critical roles in enhancing the aqueous solubility of nocathiacin I by block copolymer micelles. J. Pharm. Pharmacol. 65, 64–71.
Gao, C., Pan, J., Lu, W., Zhang, M., Zhou, L., Tian, J., 2009. In-vitro evaluation of paclitaxel-loaded MPEG-PLGA nanoparticles on laryngeal cancer cells. Anticancer Drugs 20, 807–814.
Gong, C., Deng, S., Wu, Q., Xiang, M., Wei, X., Li, L., Gao, X., Wang, B., Sun, L., Chen, Y., Li, Y., Liu, L., Qian, Z., Wei, Y., 2013. Improving antiangiogenesis and anti-tumor activity of curcumin by biodegradable polymeric micelles. Biomaterials 34, 1413–1432.
Grottkau, B.E., Cai, X., Wang, J., Yang, X., Lin, Y., 2013. Polymeric nanoparticles for a drug delivery system. Curr. Drug Metab. 14, 840–846.
Hatcher, H., Planalp, R., Cho, J., Torti, F.M., Torti, S.V., 2008. Curcumin: from ancient medicine to current clinical trials. Cell Mol. Life Sci. 65, 1631–1652.
Heard, C.M., Gallagher, S.J., Congiatu, C., Harwood, J., Thomas, C.P., McGuigan, C., Němcová, M., Nouskova, T., 2005. Preferential π–π complexation between tamoxifen and borage oil/γ linolenic acid: transcutaneous delivery and NMR spectral modulation. Int. J. Pharm. 302, 47–55.
Hiki, S., Kataoka, K., 2007. A facile synthesis of azido-terminated heterobifunctional poly(ethylene glycol)s for "click" conjugation. Bioconjugate Chem. 18, 2191–2196.
Hu, S., Zhang, Y., 2010. Endostar-loaded PEG-PLGA nanoparticles: in vitro and in vivo evaluation. Int. J. Nanomed. 5, 1039–1048.
Jia, W., Gu, Y., Gou, M., Dai, M., Li, X., Kan, B., Yang, J., Song, Q., Wei, Y., Qian, Z., 2008. Preparation of biodegradable polycaprolactone/poly(ethylene glycol)/polycaprolactone (PCEC) nanoparticles. Drug Deliv. 15, 409–416.
Jing, X., Deng, L., Gao, B., Xiao, L., Zhang, Y., Ke, X., Lian, J., Zhao, Q., Ma, L., Yao, J., Chen, J., 2014. A novel polyethylene glycol mediated lipid nanoemulsion as drug delivery carrier for paclitaxel. Nanomed. Nanotechnol. Biol. Med. 10, 371–380.

Kanazawa, T., Taki, H., Tanaka, K., Takashima, Y., Okada, H., 2011. Cell-penetrating peptide-modified block copolymer micelles promote direct brain delivery via intranasal administration. Pharm. Res. 28, 2130–2139.
Lee, H., Zeng, F., Dunne, M., Allen, C., 2005. Methoxy poly(ethylene glycol)-block-poly(delta-valerolactone) copolymer micelles for formulation of hydrophobic drugs. Biomacromolecules 6, 3119–3128.
Lee, J.H., Jung, S.W., Kim, I.S., Jeong, Y.I., Kim, Y.H., Kim, S.H., 2003. Polymeric nanoparticle composed of fatty acids and poly(ethylene glycol) as a drug carrier. Int. J. Pharm. 251, 23–32.
Letchford, K., Liggins, R., Burt, H., 2008. Solubilization of hydrophobic drugs by methoxy poly(ethylene glycol)-block-polycaprolactone diblock copolymer micelles: theoretical and experimental data and correlations. J. Pharm. Sci. 97, 1179–1190.
Maheshwari, R.K., Singh, A.K., Gaddipati, J., Srimal, R.C., 2006. Multiple biological activities of curcumin: a short review. Life Sci. 78, 2081–2087.
MaLing, G., Ke, M., HuaShan, S., MingLi, X., Juan, Z., Jia, S., JianLin, L., Yang, W., Feng, L., Xia, Z., ZhiYong, Q., 2011. Curcumin-loaded biodegradable polymeric micelles for colon cancer therapy in vitro and in vivo. Nanoscale 3, 1558–1567.
Meng, H., Xue, M., Xia, T., Ji, Z., Tarn, D.Y., Zink, J.I., Nel, A.E., 2011. Use of size and a copolymer design feature to improve the biodistribution and the enhanced permeability and retention effect of doxorubicin-loaded mesoporous silica nanoparticles in a murine xenograft tumor model. ACS Nano 5, 4131–4144.
Nair, K.L., Jagadeeshan, S., Nair, S.A., Kumar, G.S., 2011. Evaluation of triblock copolymeric micelles of delta- valerolactone and poly(ethylene glycol) as a competent vector for doxorubicin delivery against cancer. J. Nanobiotechnol. 9, 42.
Oh, J.M., Lee, S.H., Son, J.S., Khang, G., Kim, C.H., Chun, H.J., Min, B.H., Kim, J.H., Kim, M.S., 2009. Ring-opening polymerization of ε-caprolactone by poly(propyleneglycol) in the presence of a monomer activator. Polymer 50, 6019–6023.
Ono, K., Hasegawa, K., Naiki, H., Yamada, M., 2004. Curcumin has potent anti-amyloidogenic effects for Alzheimer's beta-amyloid fibrils in vitro. J. Neurosci. Res. 75, 742–750.
Rezaei, S.J., Nabid, M.R., Niknejad, H., Entezami, A.A., 2012. Folate-decorated thermoresponsive micelles based on star-shaped amphiphilic block copolymers for efficient intracellular release of anticancer drugs. Int. J. Pharm. 437, 70–79.
Shao, J., Zheng, D., Jiang, Z., Xu, H., Hu, Y., Li, X., Lu, X., 2011. Curcumin delivery by methoxy polyethylene glycol-poly(caprolactone) nanoparticles inhibits the growth of C6 glioma cells. Acta Biochim. Biophys. Sin. (Shanghai) 43, 267–274.
Shin, S.B., Cho, H.Y., Kim, D.D., Choi, H.G., Lee, Y.B., 2010. Preparation and evaluation of tacrolimus-loaded nanoparticles for lymphatic delivery. Eur. J. Pharm. Biopharm.: Off. J. Arbeitsgemeinschaft Pharmazeutische Verfahrenstechnik e. V 74, 164–171.
Shukla, A.K., Patra, S., Dubey, V.K., 2012. Nanospheres encapsulating anti-leishmanial drugs for their specific macrophage targeting, reduced toxicity, and deliberate intracellular release. Vector Borne Zoonotic Dis. 12, 953–960.
Song, Z., Feng, R., Sun, M., Guo, C., Gao, Y., Li, L., Zhai, G., 2011. Curcumin-loaded PLGA-PEG-PLGA triblock copolymeric micelles: preparation, pharmacokinetics and distribution in vivo. J. Colloid Interface Sci. 354, 116–123.
Sun, M., Zhao, L., Guo, C., Cao, F., Chen, H., Zhao, L., Tan, Q., Zhu, X., Zhu, F., Ding, T., Zhai, Y., Zhai, G., 2012. Evaluation of an oral carrier system in rats: bioavailability and gastrointestinal absorption properties of curcumin encapsulated PBCA nanoparticles. J. Nanopart. Res. 14, 1–13.
Sun, Y., Huang, Y., Bian, S., Liang, J., Fan, Y., Zhang, X., 2013. Reduction-degradable PEG-b–PAA-b–PEG triblock copolymer micelles incorporated with MTX for cancer chemotherapy. Colloids Surf. B: Biointerfaces 112, 197–203.
Tao, W., Zeng, X., Liu, T., Wang, Z., Xiong, Q., Ouyang, C., Huang, L., Mei, L., 2013. Docetaxel-loaded nanoparticles based on star-shaped mannitol-core PLGA-TPGS diblock copolymer for breast cancer therapy. Acta Biomater. 9, 8910–8920.
Tu, J., Pang, H., Yan, Z., Li, P., 2007. Ocular permeability of pirenzepine hydrochloride enhanced by methoxy poly(ethylene glycol)-poly(D,L-lactide) block copolymer. Drug Dev. Ind. Pharm. 33, 1142–1150.
Wang, H., Zhao, Y., Wu, Y., Hu, Y.L., Nan, K., Nie, G., Chen, H., 2011. Enhanced anti-tumor efficacy by co-delivery of doxorubicin and paclitaxel with amphiphilic methoxy PEG-PLGA copolymer nanoparticles. Biomaterials 32, 8281–8290.
Wang, Y., Wang, C., Gong, C., Guo, G., Luo, F., Qian, Z., 2012. Polysorbate 80 coated poly(varepsilon-caprolactone)-poly(ethylene glycol)-poly(varepsilon-caprolactone) micelles for paclitaxel delivery. Int. J. Pharm. 434, 1–8.
Wei, Y., Wang, Y., Kang, A., Wang, W., Ho, S.V., Gao, J., Ma, G., Su, Z., 2012. A novel sustained-release formulation of recombinant human growth hormone and its pharmacokinetic, pharmacodynamic and safety profiles. Mol. Pharm. 9, 2039–2048.
Xie, X., Tao, Q., Zou, Y., Zhang, F., Guo, M., Wang, Y., Wang, H., Zhou, Q., Yu, S., 2011. PLGA nanoparticles improve the oral bioavailability of curcumin in rats: characterizations and mechanisms. J. Agric. Food Chem. 59, 9280–9289.
Yallapu, M.M., Jaggi, M., Chauhan, S.C., 2010. Beta-cyclodextrin-curcumin self-assembly enhances curcumin delivery in prostate cancer cells. Colloids Surf. B: Biointerfaces 79, 113–125.
Yen, F.L., Wu, T.H., Tzeng, C.W., Lin, L.T., Lin, C.C., 2010. Curcumin nanoparticles improve the physicochemical properties of curcumin and effectively enhance its antioxidant and antihepatoma activities. J. Agric. Food Chem. 58, 7376–7382.
Yin, H.T., Zhang, D.G., Wu, X.L., Huang, X.E., Chen, G., 2013. In vivo evaluation of curcumin-loaded nanoparticles in a A549 xenograft mice model. Asian Pac. J. Cancer Prev. 14, 409–412.
Zhang, P., Wu, H., Wu, H., Lu, Z., Deng, C., Hong, Z., Jing, X., Chen, X., 2011. RGD-conjugated copolymer incorporated into composite of poly(lactide-co-glycotide) and poly(L-lactide)-grafted nanohydroxyapatite for bone tissue engineering. Biomacromolecules 12, 2667–2680.
Zhang, Y., Li, X., Zhou, Y., Wang, X., Fan, Y., Huang, Y., Liu, Y., 2010a. Preparation and evaluation of poly(ethylene glycol)-poly(lactide) micelles as nanocarriers for oral delivery of cyclosporine a. Nanoscale Res. Lett. 5, 917–925.
Zhang, Y., Tang, L., Sun, L., Bao, J., Song, C., Huang, L., Liu, K., Tian, Y., Tian, G., Li, Z., Sun, H., Mei, L., 2010b. A novel paclitaxel-loaded poly(epsilon-caprolactone)/Poloxamer 188 blend nanoparticle overcoming multidrug resistance for cancer treatment. Acta Biomater. 6, 2045–2052.
Zobel, H.P., Stieneker, F., Atmaca-Abdel Aziz, S., Gilbert, M., Werner, D., Noe, C.R., Kreuter, J., Zimmer, A., 1999. Evaluation of aminoalkylmethacrylate nanoparticles as colloidal drug carrier systems. Part II: characterization of antisense oligonucleotides loaded copolymer nanoparticles. Eur. J. Pharm. Biopharm.: Off. J. Arbeitsgemeinschaft Pharmazeutische Verfahrenstechnik e. V 48, 1–12.